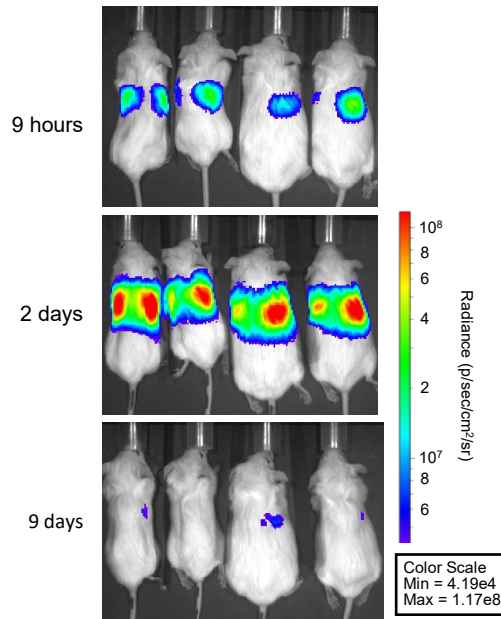


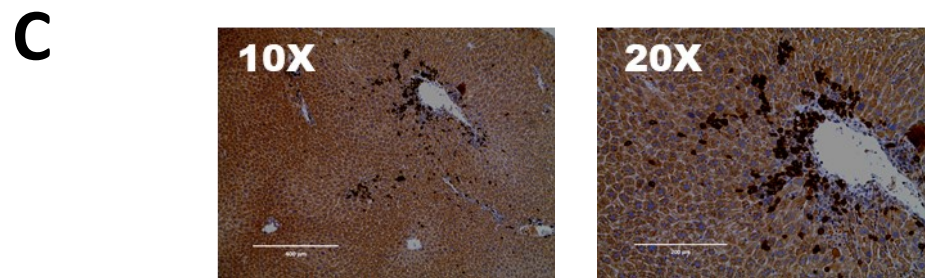
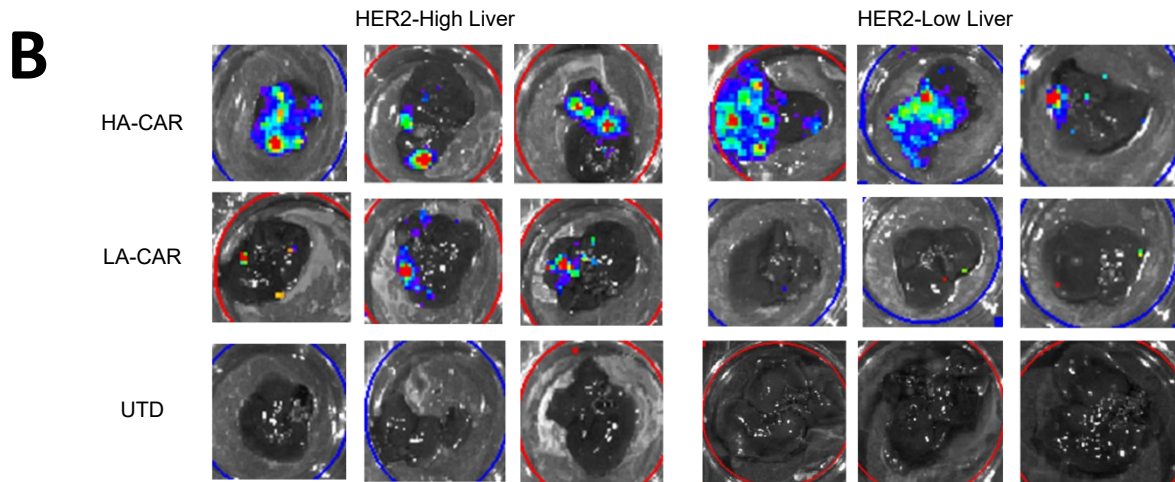
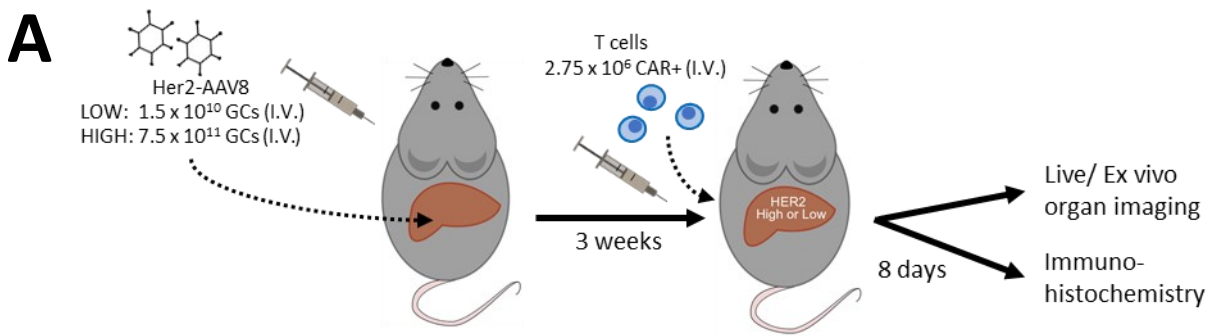
A rational mouse model to detect on-target off-tumor CAR T cell toxicity

Mauro Castellarin¹, Caroline Sands¹, Tong Da¹, John Scholler¹, Kathleen Graham¹, Elizabeth Buza², Joseph A. Fraietta^{1,3}, Yangbing Zhao^{1,4}, Carl H. June^{1,4,*}

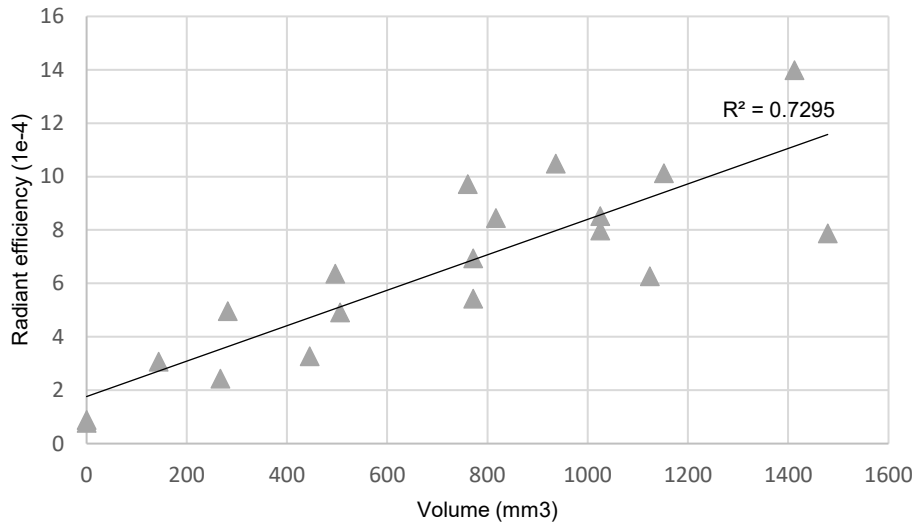
JCI Insight Supplemental Figures



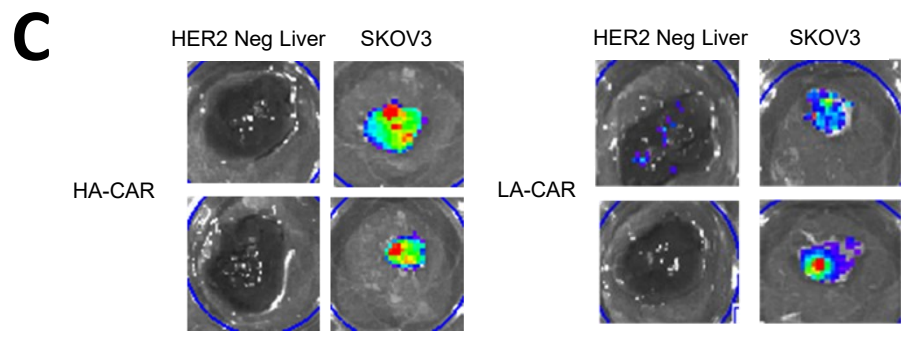
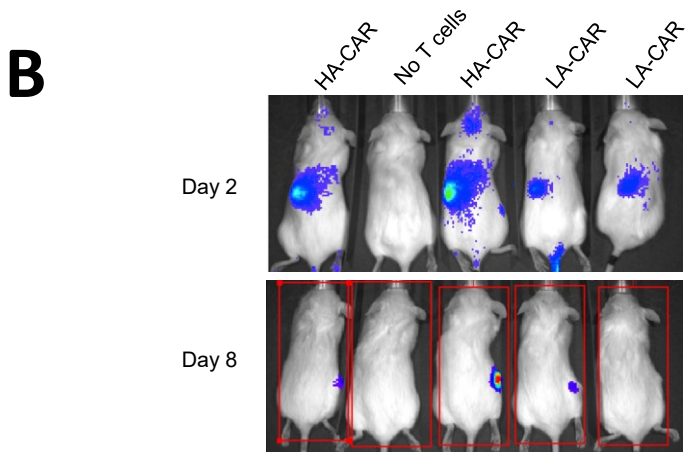
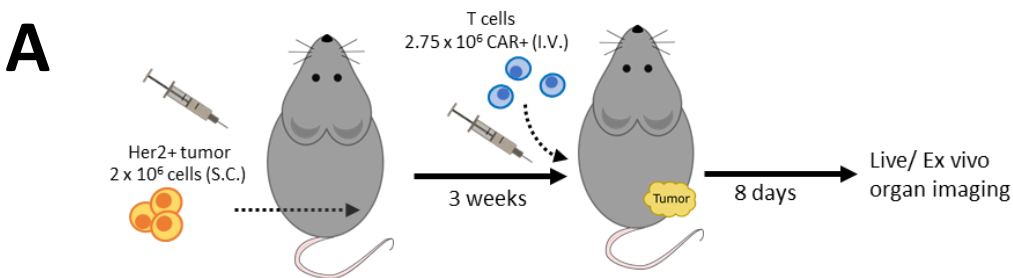
Supplemental Figure 1. Transient luciferase expression following hydrodynamic tail IV injection. Mice (n = 4) were injected with 10ug of the luciferase vector shown in Supplemental Figure 5C by hydrodynamic tail vein injection and then in vivo expression was detected by IVIS imaging at the times indicated.



Supplemental Figure 2. Her2 CAR T cell liver infiltration is dependent on CAR affinity and antigen expression. (A) NSG mice ($n = 3$ per group) were injected with either high low or low GCs of human Her2 AAV8 to obtain hepatic Her2 expression. The mice were then injected with human T cells that expressed luciferase and either a high or low-affinity (HA or LA, respectively) Her2 CAR. **(B)** Ex vivo bioluminescent imaging of luciferase-expressing HA and LA CAR T cells in Her2 high-expressing mouse livers. **(C)** CD8+ T cell infiltration was detected by IHC in a hepatic Her2 high mouse with HA CAR T cells, which is representative of the group ($n = 3$) (Scale bars, 400 μm for 10X magnification and 200 μm for 20X magnification).



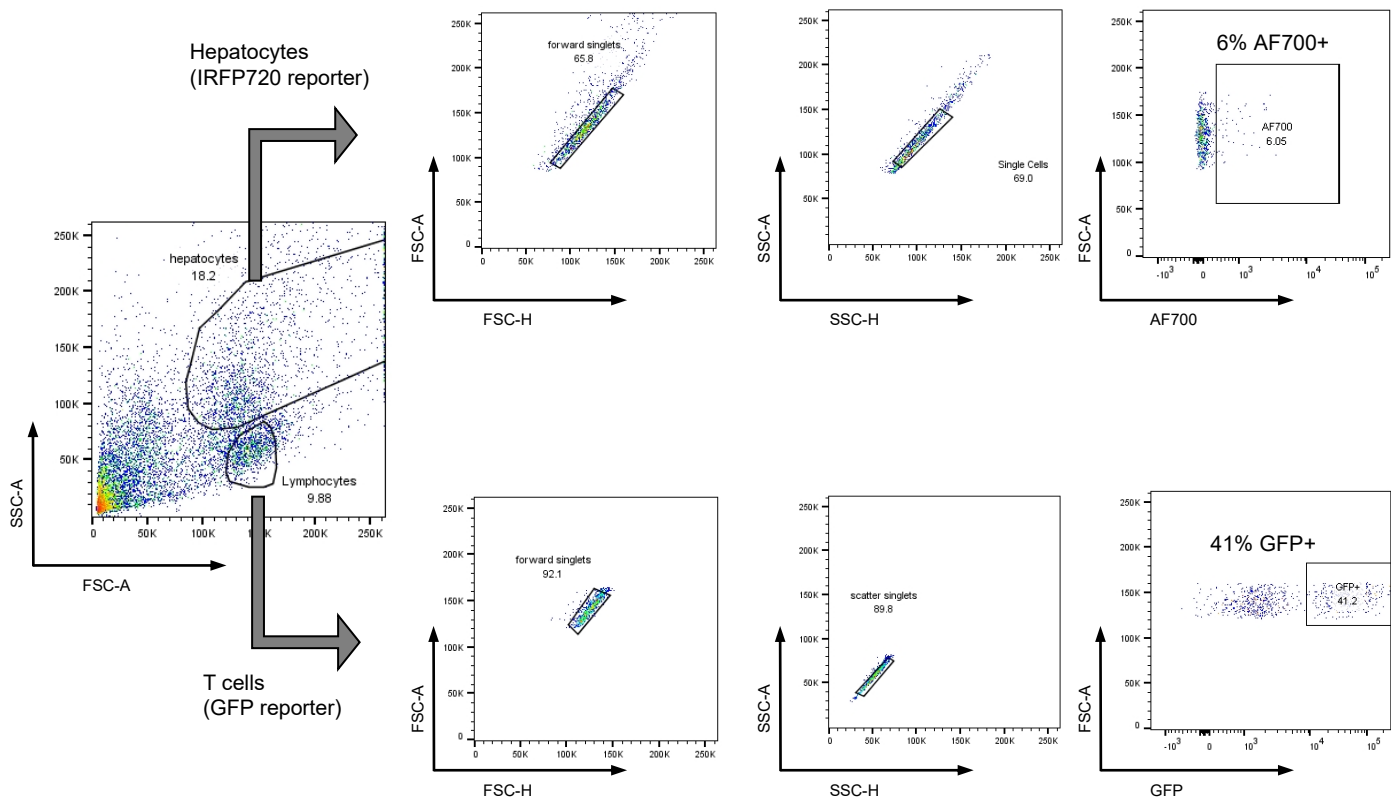
Supplemental Figure 3. Tumor measurement comparison between calipers versus radiance. The subcutaneous SKOV3 tumor xenografts shown in Figure 5 were regularly measured for size by both caliper measurements and by IVIS imaging of the fluorescent reporter, IRFP720. The two types of measurements were compared for concordance in n= 18 mice.



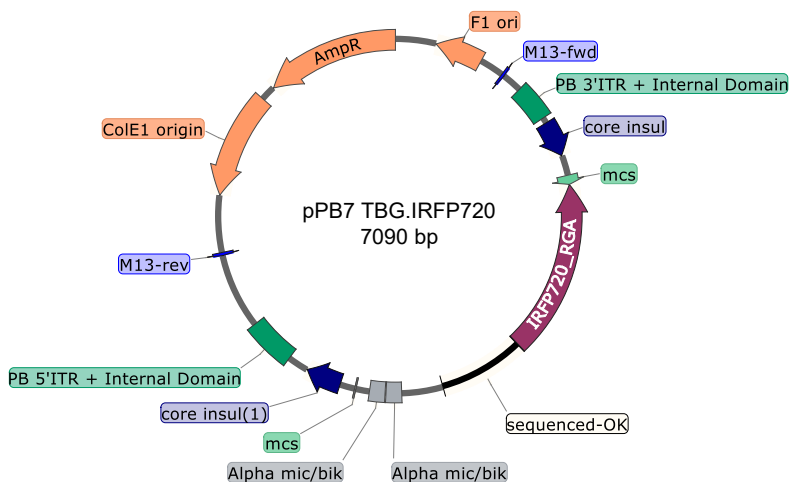
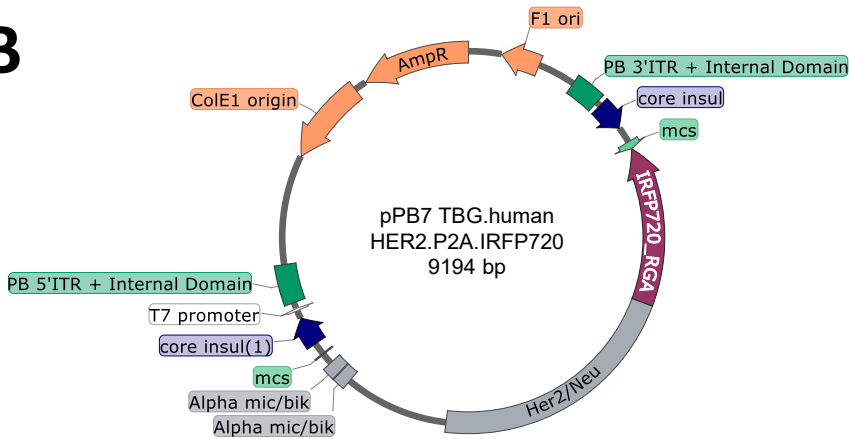
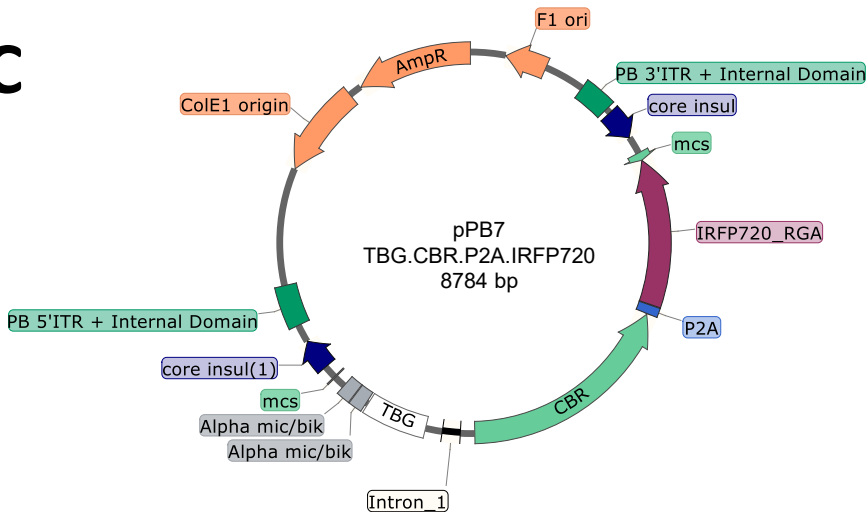
Supplemental Figure 4. High and low-affinity HER2 CAR T cells exhibit similar trafficking to tumor in mice without hepatic Her2 expression. (A) NSG mice were engrafted with subcutaneous Her2+ SKOV3 tumor cells. The mice were then injected with human T cells that expressed luciferase and either a high or low-affinity (HA or LA, respectively) Her2 CAR. **(B)** In vivo bioluminescent imaging of mice (n = 2) showed T cells predominantly in the spleen at day 2 and in the tumor by day 8 for both the HA and LA CAR T cells. **(C)** Ex vivo bioluminescent imaging of the liver and tumor (n = 2).



Supplemental Figure 5. Vector maps of customized viral vectors. The AAV8 vectors used to transduce hepatocytes included a GFP-only control vector (**A**) and a vector that contained both a human Her2 gene and a fluorescent reporter (**B**). The lentiviral vectors used to transduce T cells included a luciferase with GFP control vector (**C**) a luciferase and high-affinity Her2 CAR vector (**D**) and a luciferase and low-affinity Her2 CAR vector (**E**).



Supplemental Figure 6. Flow cytometry gating strategy for dissociated and isolated hepatocytes and T cells. Mice were hydrodynamically injected with plasmid DNA, pPB7 TBG.IRFP720 and after a minimum of 24 hours the livers were harvested, and hepatocytes were dissociated. Human T cells that expressed eGFP were then added to the liver homogenate prior to debris removal. The cells were then analyzed on a BD LSRFortessa flow cytometer to determine a gating strategy for detecting IRFP720+ hepatocytes as shown in Figure 1G.

A**B****C**

Supplemental Figure 7. Vector maps of customized piggyBac transposon vectors. The piggyBac transposase vector, pCMV-hyPBase was obtained from the Wellcome Trust Sanger Institute. The piggyBAC transposon plasmid, PB007 SPB-007 (transposagen) was used as the parental vector to make the following constructs: **(A)** pPB7 TBG.IRFP720. **(B)** pPB7 TBG.human Her2.P2A.IRFP720. **(B)** pPB7 TBG.CBR.P2A.IRFP720.

Supplemental Table 1. Summary of post-mortem pathology report on mouse livers.

Mouse ID	Her2-AAV8 GC dose	scFv affinity of CAR	Liver Assessment	Scale
3052	High	Low	Severe diffuse hepatocellular degeneration, regeneration, and multifocal single hepatocellular necrosis with extensive lobular collapse and oval cell hyperplasia	4
			Moderate multifocal lymphocytic portal infiltrates	3
			Moderate multifocal extramedullary hematopoiesis	3
3053	High	High	Marked bridging to massive subacute hepatocellular necrosis, degeneration, and regeneration with fibroplasia (presumptive), extensive lobular collapse, bile duct and oval cell hyperplasia	5
3054	High	High	Marked bridging to massive subacute hepatocellular necrosis, degeneration, and regeneration with fibroplasia (presumptive), extensive lobular collapse, bile duct and oval cell hyperplasia	5
3025	Low	High	Severe multifocal perivascular (portal and centrilobular) and sinusoidal lymphocytic infiltrates with rare single hepatocellular necrosis	4
3028	Low	High	Severe multifocal perivascular (portal and centrilobular) and sinusoidal lymphocytic infiltrates with occasional single hepatocellular necrosis	4
3091	Low	High	Mild multifocal perivascular (portal and centrilobular) and sinusoidal lymphocytic infiltrates with rare single hepatocellular necrosis	2

Scale:

- 0 – WNL
- 1 – Minimal
- 2 – Mild
- 3 – Moderate
- 4 – Severe
- 5 – Marked